RSC Advances

ROYAL SOCIETY OF CHEMISTRY

www.rsc.org/advances

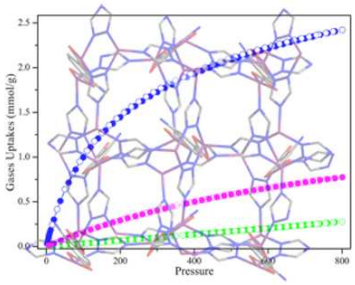

An polyhedra porous MOF, with high selectivity of CO_2 over, being formed by TRZ-Zn layer connected ATPA linker.

Formation of a Metal-Organic Framework with High Gases Uptakes Based upon Amino-Decorated Polyhedral Cages

Ruirui Yun*, [a] Ranran Cui,[a] Fujun Qian,[a] Xiaoyan Cao,[a] Shizhong Luo,[a] and Baishu Zheng*[b]

Abstract A new three-dimensional metal-organic framework **1** was solvothermally synthesized by 1,2,4-triazole and 2-aminoterephthalic acid, and structurally characterized. **1** features a three-dimensional structure with one-dimensional pores along the c axis of 6 × 6 $Å^2$. The activated **1** exhibits H_2 uptake capacity at 77 K. Importantly, it shows excellent enthalpy of CO_2 (35 kJ/mol) and methane (24 kJ/mol), compared to previous porous materials.

Introduction

Metal-organic frameworks (MOFs), a subclass of porous materials with high surface area, diversity and modifiability, are particularly attractive synthetic targets due to their fundamental interest and potential applications.[1] One such application is the sequestration of CO_2 emitted from industrial flue streams. In this case, low-cost porous materials capable of physisorption of CO_2 are idea candidates due to the process requires less energy for adsorbent regeneration.[2] Therefore, CO_2 capture from industrial process through MOFs has been highly investigated in recent years.[3]

To enhance CO_2 adsorption capacity and selectivity, various strategies have been explored in MOFs construction.[2c, 4] One of the most promising strategies to increase the uptake capacity is the deliberate enhancement of the adsorbent-adsorbate interactions. For example, the incorporation of alkylamine functionality within the pores of MOFs offers a significant opportunity to produce highly efficient capture materials by virtue of the affinity of alkylamines for CO_2. Furthermore, the suitable pore size commensurate with the size of the gas molecule can also be critical because large cavities do not necessarily lead to a high uptake capacity for small gas molecules such as CO_2, CH_4 and H_2.

With these consideration in mind and our previous studies on carbon capture and sequestration (CCS) and gas storage,[5] in this contribution, we reported an exceptional low-cost pillar layer MOF, $[Zn_2(TRZ)_2(ATPA)]\cdot G$ (TRZ = 1,2,4-triazole, ATPA = 2-aminoterephthalic acid, G = guest molecules), that integrates multiple desirable features such as framework functionalization by amino groups and moderate nanoscopic polyhedral cages. The triangular TRZ ligand was selected because its multiple coordination modes allow for the construction of topologically diverse structure and the linear dicarboxylate ATPA ligand was selected because of the potential of the amine group to interact with CO_2 molecules. As expected, the coassembly between triangular TRZ, linear ATPA ligands and Zn nuclear led to the formation of a new **fsx** topology framework with amino-decorated polyhedral cages. In addition, to the best of our knowledge, **1** exhibits higher enthalpy of CO_2 (34 kJ/mol) among known MOFs with amino-modified. Impressively, it is shown here that it exhibits highest CO_2/N_2 selectivity ratio (S = 44 at 273 K) compared with pillar layer MOFs.

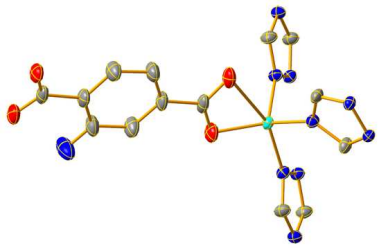

Figure1. view of 1. five coordination of Zn-centre (Red: Oxygen atom; green: Zn atom; blue: N atom).

[a]*The Key Laboratory of Functional Molecular Solids, Ministry of Education, Anhui Key Laboratory of Functional Molecular Solids, Anhui Laboratory of Molecule-Based Materials, College of Chemistry and Materials Science, Anhui Normal University, Wuhu 241000 PRC. E-mail: yunruirui@gmail.com*

[b]*School of Chemistry and Chemical Engineering, Hunan University of Science and Technology, Xiangtan 411201, PRC*

Experimental section

General information

All starting materials and solvent, unless otherwise noted, were obtained from Alfa Aesar Organics and used without further purification. Elemental analyses (C, H, and N) were carried out on a Perkin-Elmer 240 analyzer. The IR spectra were obtained on a VECTOR TM 22 spectrometer with KBr pellets in the 4000~400 cm^{-1} region. ^1H NMR spectra were recorded on a Bruker DRX-500 spectrometer with tetramethylsilane as an internal reference. Thermal gravimetric analyses (TGA) were performed under N_2 atmosphere (100 ml/min) with a heating rate of 5 °C/min using a 2960 SDT thermogravimetric analyzer. Powder X-ray diffraction (PXRD) data were collected on a Bruker D8 ADVANCE X-ray diffractometer using Cu Kα radiation (λ = 1.5418 Å) at room temperature with a routine power of 1600 W (40 kV, 40 mA) in a scan speed of 5º/min and a step size of 0.02 in 2θ. The simulated PXRD spectra were acquired by the diffraction-crystal module of the *Mercury* program based on the single crystal data. The program is available free of charge *via* internet at *http://www.iucr.org*.

Preparation of 1.

$Zn(NO_3)_2 \cdot 6H_2O$ (0.1 mmol, 29.8 mg), 1,2,4-triazole (0.025 mmol, 2 mg), 2-aminoterephthalic acid (0.025 mmol, 4.5 mg) were dissolved in a mixed solvent of DMF (2 ml) and H_2O (0.5 ml), then 0.025 ml HNO_3 with a concentration of 62% was added, and the mixture was transferred to and sealed in a 20 ml Teflon-lined autoclave, which was heated at 90 °C for 48 h. After slow cooling to room temperature, colourless crystals of **1** were collected by filtration. Anal. Calcd (Found) for activated **1**, $C_{12}H_9O_4N_7Zn_2$: C, 32.31 (33.53); H, 2.03 (2.15); N, 21.98 (22.17) %.

Single crystal X-ray study

Single-crystal X-ray diffraction data were measured on a Bruker Smart Apex CCD diffractometer at 293 K using graphite monochromated Mo/Kα radiation (λ = 0.71073 Å). Data reduction was made with the Bruker Saint program. The crystal of **1** was mounted in a flame sealed capillary, containing a small amount of mother liquor to prevent desolvation during data collection, and data were collected at 293K. The structures were solved by direct methods and refined with full-matrix least squares technique using the SHELXTL package.[6] Non-hydrogen atoms were refined with anisotropic displacement parameters during the final cycles. Organic hydrogen atoms were placed in calculated positions with isotropic displacement parameters set to 1.2×Ueq of the attached atom. The hydrogen atoms of the ligand and water molecules could not be located, but are included in the formula. The unit cell of **1** include a large region of disordered solvent molecules, which could not be modeled as discrete atomic sites. The SQUEEZE subroutine of the PLATON software suite[7] was applied to remove the scattering from the highly disordered solvent molecules due to the guest solvent molecules are highly disordered and impossible to refine using conventional discrete-atom models. Structure information of **1** was deposited at the Cambridge Crystallographic Data Center (CCDC reference numbers was: 1020282). Crystal data and further information on the structure determination are summarized in Table S1.

Sample activation

As-synthesized **1** crystals were immersed in anhydrous acetone for 3 days to remove the nonvolatile solvates (DMF and water), the extract was decanted every 8 h, and fresh anhydrous acetone was replaced. After the removal of acetone by decanting, the sample was further activated by drying under a dynamic high vacuum at 90 °C overnight to obtain the desolvated sample.

Gas adsorption experiments

In the gas sorption measurements, all of the gases used are of 99.999% purity. Low-pressure N_2 (at 77 K) and CO_2 (273 K) adsorption measurements (up to 1 bar) were performed on Micromeritics ASAP 2020 M+C surface area analyzer. For all low-pressure isotherms, warm and cold free space correction measurements were performed using ultra-high-purity He gas (UHP grade 5.0, 99.999% purity).

Results and discussion

Crystal structure description

Single-crystal X-ray diffraction reveals that **1** crystallizes in the centrosymmetric space group P4/ncc. As shown in Figure 1, each metal centre of **1** is five-coordinated,

binding to three nitrogen atoms which from different TRZ molecules and two oxygen atoms from ATPA molecule. Because of the tow oxygen atoms from ATPA were chelated, therefore, the coordination configuration of Zn-centre can be described as a pyramid. Interestingly, as illustrated by an eight-cycle layer in figure 2, four TRZ ligands coordinated with four Zn atoms to form a 6 × 6 Å window in the one-dimensional TRZ-Zn layer (Figure 2a) which was further linked with the second ATPA ligand just like the pillars to binding a three-dimensional pillar-layer framework.

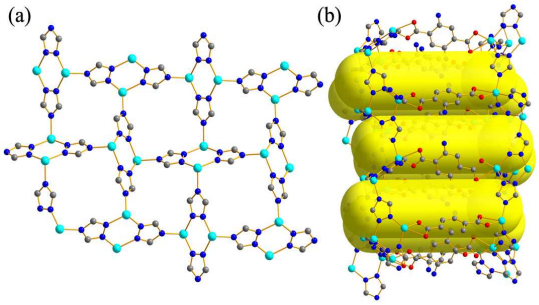

Figure2. (a) one-dimensional TRZ-Zn layer; (b) three-dimensional framework of 1 which come from TRZ-Zn layer binding to ATPA ligands.

The overall structure of **1** consists of TRZ-Zn-TRZ octatomic ring layer, which like a zeolite window, and ATPA as pillar which can be called 3-D framework (Figure 3). For easy comprehension, we simplified TRZ ligand and Zn atoms as three- and four-connected nodes, respectively. Notably, the ATPA ligand as pillar connects the octatomic ring layer. Consequently, the integrate framework of **1** is assigned with the reticular chemistry structure resource (RCSR) symbol **fsx**. For the above reasons, TRZ, ATPA ligands and Zn-centre forms the unprecedented hybrid coordination polyhedral cages which were filled with guest molecules. The void space accounts for approximately 45.4 % of the whole crystal volume (2243.8 out of the 4946.68 per unit cell volume) by PLATON analysis.

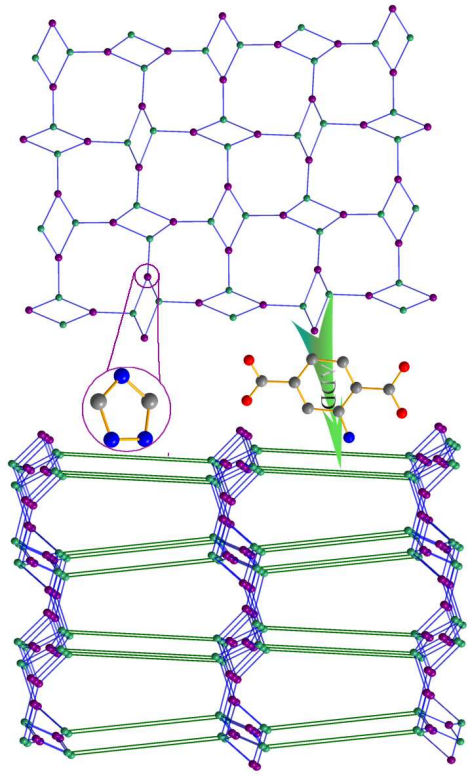

Figure3. Topologic network of 1 (2-D layer forms 3-D framework when the ATPA as the pillar)**.**

Thermogravimetric Analysis and gas adsorption properties

Thermogravimetric analysis shows that the removal of solvent molecules occurs in the temperature range of (60-200 ºC) and there is no further weight loss up to ~300 ºC (Figure S3). The architectural stability and permanent porosity of **1** were also confirmed by gas adsorption studies (N_2, H_2, CH_4 and CO_2) on a Micrometritics ASAP 2020 surface area and pore size analyzer. As shown in Figure 4, **1** exhibits a type-I adsorption isotherm typical of porous material of permanent micro porosity. Based on the N_2 (77 K) adsorption isotherm, the surface area of activated 1 calculated from the Langmuir equation is about 700 $m^2 \cdot g^{-1}$ and the corresponding BET surface area is 477 $m^2 \cdot g^{-1}$. The median pore size of 5.2 Å (using Horvath-Kawazoe method) and micropore volume of 0.210 $cm^3 \cdot g^{-1}$were also calculated which consistent with the total framework pore volume (0.35 $cm^3 \cdot g^{-1}$) derived from the X-ray crystal structure of **1**.

Furthermore, H_2 uptakes have been measured at 77 and 87 K, due to H_2 is considered as an ideal energy source

candidate in the future which possess higher powder density than other fuel such as methane and gasoline. We can see from Figure 4, **1** exhibits a high total H_2 uptake capacity of 1.1 wt% at 77 K and 1 bar, which among higher H_2 uptakes at low pressure. Isosteric heat (Q_{st}) of H_2 adsorption is estimated to be 7.87 kJ·mol^{-1} at zero coverage, which is highest compared with other pillar layer porous materials (Figure S2).[8] Adsorption behaviour of **1** towards CH_4 was studied at 273 and 298 K. The amount of CH_4 uptake at 273 and 298 K (1.0 bar) is 1.16 and 0.75 mmol·g^{-1}, respectively. CH_4 sorption Q_{st} is estimated to be 24.3 kJ·mol^{-1} at zero loading which is higher value among reported MOFs.[9] Impressively, CO_2 and N_2 low-pressure adsorption-desorption isotherms were measured at 273 and 298 K (0-1.0 bar). At 273 K, the uptake amount of CO_2 is 43.6 cm·g^{-1} (STP, 1.95 mmol·g^{-1}) at 0.15 bar. In contrast, its N_2 adsorption is very lower of 5.0 cm·g^{-1} (STP, 0.22 mmol·g^{-1}) at 273 K and 0.75 bar. As shown in Figure 5, the selectivity of 1 is 44 and 27 at 273 K and 298 K, respectively, which is calculated from the pure-component isotherms by dividing the mass of CO_2 adsorbed at 0.15 bar and N_2 adsorbed at 0.75 bar according the equation 3 (we have mentioned ESI). As far as we known, it is the highest record for pillar layer MOFs materials, indicating that **1** may be an excellent candidate for the postcombustion capture of CO_2.[10]

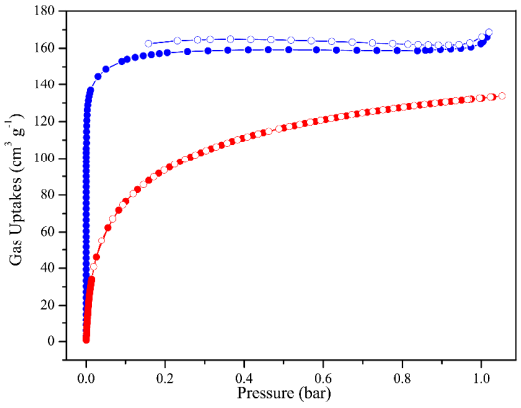

Figure 4. N_2 and H_2 adsorption isotherms of **1** (blue, N_2; red, H_2; filled circles, adsorption; empty circles, desorption).

To better understand the observations and evaluate the extent of CO_2-framework interactions, the isosteric heat (Q_{st}) of CO_2 adsorption was calculated by the virial method using experimental isotherm data at 273 and 298 K. The adsorption enthalpy for **1** is ca. 35 kJ·mol^{-1} at zero loading, which reflects a strong adsorbent-adsorbate interaction (Figure S2). The higher Q_{st} value in **1** may be attributed to the existence of amino-modified framework and moderate pore size.

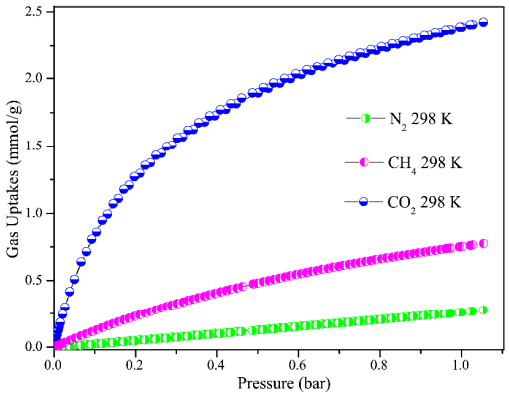

Figure 5. The sorption isotherms of CO_2, CH_4 and N_2 on 1 at 298 K (blue: CO_2; magenta: CH_4; green: N_2).

Conclusion

In summary, we have synthesized a novel amine functionalized porous metal-organic framework **1** with **fsx** topology and nanoscopic polyhedral cages. It exhibits higher enthalpy of CO_2 among the reported pillar layer porous materials. Impressively, it shows highest selective separation of CO_2 over N_2 due to its functionalized amine groups in the framework and moderate pore size. The realization of this example of low-cost amino-modified pillar layer framework for highly selective separation of CO_2/N_2 might facilitate the extensive research endeavour to explore this MOF approach, so some novel amino-modified MOF materials will be emerging for capturing carbon from industrial flue.

Acknowledgements

We thank the support of this work by the NSFC (21401004), Talent Cultivation Fund of Anhui Normal University (711335), the Doctoral Scientific Research Foundation (070138), and the Natural Science Foundation of Anhui Province (1408085ME83).

Appendix A. Supplementary data

Supplementary material CCDC 1020282 contain the supplementary crystallographic data for **1**. These data can

be obtained free of charge from The Cambridge Crystallographic Centre via www.ccdc.cam.ac.uk/data-request/cif.

Notes and references

1 (a) J. B. DeCoste, G. W. Peterson, *Chem. Rev.* 2014, **114**, 5695; (b) M. Li, D. Li, M. O'Keeffe, O. M. Yaghi, *Chem. Rev.* 2014, **114**, 1343; (c) Q. Y. Yang, D. H. Liu, C. L. Zhong, J. R. Li, *Chem. Rev.* 2013, **113**, 8261; (d) H. Park, D. M. Moureau, J. B. Parise, *Chem. Mater.* 2006, **18**, 525.

2 (a) J. A. Mason, K. Sumida, Z. R. Herm, R. Krishna, J. R. Long, *Energy Environ. Sci.* 2011, **4**, 3030; (b) J. J. Perry, J. A. Perman, M. J. Zaworotko, *Chem. Soc. Rev.* 2009, **38**, 1400; (c) B. S. Zheng, J. Bai, J. G. Duan, L. Wojtas, M. J. Zaworotko, *J. Am. Chem. Soc.* 2011, **133**, 748.

3 (a) O. K. Farha, C. E. Wilmer, I. Eryazici, B. G. Hauser, P. A. Parilla, K. O'Neill, A. A. Sarjeant, S. T. Nguyen, R. Q. Snurr, J. T. Hupp, *J. Am. Chem. Soc.* 2012, **134**, 9860; (b) R. R. Yun, J. G. Duan, J. Bai, Y. Z. Li, *Cryst. Growth Des.* 2013, **13**, 24; (c) D. M. D'Alessandro, B. Smit, J. R. Long, J. R. *Angew. Chem., Int. Ed.* 2010, **49**, 6058.

4 (a) A. Demessence, D. M. D'Alessandro, M. L. Foo, J. R. Long, *J. Am. Chem. Soc.* 2009, **131**, 8487; (b) E. Haldoupis, S. Nair, D. S. Sholl, *J. Am. Chem. Soc.* 2012, **134**, 4313.

5 (a) R. R. Yun, Z. Y. Lu, Y. Pan, X. Z. You, J. Bai, *Angew. Chem. Int. Ed.* 2013, **52**, 11282; (b) Z. X. Wang, B. S. Zheng, H. T. Liu, X. Lin, X. Y. Yu, P. G. Yi, R. R. Yun, *Cryst. Growth&Des.* 2013, **13**, 5001; (c) Z. X. Wang, B. S. Zheng, H. T. Liu, P. G. Yi, X. F. Li, X. Y. Yu, R. R. Yun, *Dalt. Trans.* 2013, **42**, 11304p; (d) R. R. Yun, Y. Q. Jiang, S. Z. Luo, C. Chen, *RSC Adv.* 2014, **4**, 36845.

6 (a) G. M. Sheldrick, SHELXS-97, Program for the Solution of Crystal Structures, University of Göttingen, Göttingen (Germany) 1997. See also: Sheldrick GM *Acta Crystallogr. A* 1990, **46**, 467; (b) G. M. Sheldrick, SHELXL-97, Programfor the Refinement of Crystal Structures,University ofGöttingen, Göttingen (Germany) 1997. See also: G. M. Sheldrick, *Acta Crystallogr. A* 2008, **64**, 112.

7 A. L. Spek, *J. Appl. Crystallogr.*, 2003, **36**, 7.

8 (a) P. Song, B. Liu, Y. Q. Li, J. Z. Yang, Z. M. Wang, X. G. Li, *CrystEngComm*, 2012, **14**, 2296; (b) S. S. Sen, S. Neogi, A. Aijaz, Q. Xu, P. K. Bharadwaj, *Inorg. Chem.* 2014, **53**, 7591.

9 (a) X. S. Wang, S. Ma, K. Rauch, J. M. Simmons, D. Yuan, X. Wang, T. Yildirim, W. C. Cole, J. Lopez, A. D. Meijere, H. C. Zhou, *Chem. Mater.* 2008, **20**, 3145; (b) X. Duan, J. C. Yu, J. F. Cai, Y. B. He, C. D. Wu, W. Zhou, T. Yildirim, Z. Zhang, S. C. Xiang, M. O'Keeffe, B. L. Chen, G. D. Qian, *Chem. Commun.* 2013, **49**, 2043; (c) Z. J. Zhang, Z. Z. Yao, S. C. Xiang, B. L. Chen, *Energy Environ. Sci.,* 2014, **7**，2868.

10 (a) M. Pera-Titus, *Chem. Rev.* 2014, **114**, 1413; (b) D. M. D'Alessandro, B. Smit, J. R. Long, *Angew. Chem. Int. Ed.* 2010, **49**, 6058; (c) P. Nugent, Y. Belmabkhout, S. D. Burd, A. J. Cairns, R. Luebke, K. Forrest, T. Pham, S. Q. Ma, B. Space, L. Wojtas, M. Eddaoudi, M. J. Zaworotko, *Nature* 2013, **495**, 7439.